



1 **Atmospheric mercury in the southern hemisphere – Part 1: Trend and inter-**  
2 **annual variations of atmospheric mercury at Cape Point, South Africa, in 2007**  
3 **-2017, and on Amsterdam Island in 2012 - 2017**

4  
5 Franz Slemr<sup>1</sup>, Lynwill Martin<sup>2</sup>, Casper Labuschagne<sup>2</sup>, Thumeka Mokolo<sup>2</sup>, H  l  ne Angot<sup>3</sup>,  
6 Olivier Magand<sup>4</sup>, Aur  lien Dommergue<sup>4</sup>, Philippe Garat<sup>5</sup>, Michel Ramonet<sup>6</sup>, Johannes Bieser<sup>7</sup>

7  
8 Corresponding author: [Franz.Slemr@mpic.de](mailto:Franz.Slemr@mpic.de)  
9 Second corresponding author: [Lynwill.Martin@weathersa.co.za](mailto:Lynwill.Martin@weathersa.co.za)

10  
11  
12 <sup>1</sup>Max-Planck-Institut f  r Chemie (MPI), Air Chemistry Division, Hahn-Meitner-Weg 1, D-55128 Mainz,  
13 Germany

14 <sup>2</sup>South African Weather Service c/o CSIR, P.O.Box 320, Stellenbosch 7599, South Africa

15 <sup>3</sup>Institute of Arctic and Alpine Research, University of Colorado Boulder, Boulder, CO, USA

16 <sup>4</sup>Institut des G  osciences de l'Environnement, Univ Grenoble Alpes, CNRS, IRD, Grenoble INP, 38400  
17 Grenoble, France

18 <sup>5</sup>LJK, Univ Grenoble Alpes, CNRS, IRD, Grenoble INP, 38401 Grenoble, France

19 <sup>6</sup>Laboratoire des Sciences du Climat et de l'Environnement, LSCE-IPSL (CEA-CNRS-UVSQ), Universit    
20 Paris-Saclay, 91191 Gif-sur-Yvette, France

21 <sup>7</sup>Helmholtz-Zentrum Geesthacht (HZG), Institute of Coastal Research, Max-Planck-Str. 1, D-21502  
22 Geesthacht, Germany

23

24

25

26

27 **Abstract**

28 The Minamata Convention on mercury (Hg) entered into force in 2017, committing its 116 parties (as  
29 of January 2019) to curb anthropogenic emissions. Monitoring of atmospheric concentrations and  
30 trends is an important part of the effectiveness evaluation of the Convention. A few years ago (in 2017)  
31 we reported an increasing trend of atmospheric Hg concentrations at the Cape Point Global  
32 Atmospheric Watch (GAW) station in South Africa (34  21'S, 18  29'E) for the 2007 – 2015 period. With



33 2 more years of measurements at Cape Point and the 2012 – 2017 data from Amsterdam Island  
34 (37°48'S, 77°34'E) in the remote southern Indian Ocean, a more complex picture emerges: at Cape  
35 Point the upward trend for the 2007 – 2017 period is still significant but none or slightly downward  
36 trend was detected for the period 2012 – 2017 both at Cape Point and Amsterdam Island. The upward  
37 trend at Cape Point is thus driven mainly by the 2007 - 2014 data. Using ancillary data on <sup>222</sup>Rn, CO, O<sub>3</sub>,  
38 CO<sub>2</sub>, and CH<sub>4</sub> from Cape Point and Amsterdam Island the possible reasons for the trend and its change  
39 are investigated. In a companion paper this analysis is extended for the Cape Point station by  
40 calculations of source and sink regions using backward trajectory analysis.

## 41 1 Introduction

42 Mercury (Hg) is an environmental toxicant emitted by both natural and anthropogenic sources – the  
43 latter regulated by the Minamata Convention. This Convention, which entered into force in August  
44 2017, requires periodic effectiveness evaluation (Article 22) to ensure that it meets its objectives. This  
45 evaluation will be based on a combination of Hg monitoring data, including levels of Hg and Hg  
46 compounds in air, biota, and humans. A few years ago, we reported an upward trend of atmospheric  
47 mercury concentrations at the Cape Point Global Atmospheric Watch (GAW) station at Cape Point  
48 (CPT, 34°21'S, 18°29'E) in South Africa for the 2007 – 2015 period (Martin et al., 2017). An upward  
49 trend was surprising because manual mercury measurements at the same site in 1995 – 2004 showed  
50 a downward trend. Downward trends of atmospheric mercury concentrations and of mercury wet  
51 deposition have also been reported for many sites in the northern hemisphere (Temme et al., 2007;  
52 Cole et al., 2014; Steffen et al., 2015; Weigelt et al., 2015; Weiss-Penzias et al., 2016; Marumoto et al.,  
53 2019) but Cape Point has been the only station in the southern hemisphere with a long enough  
54 mercury concentration record to calculate trends. The northern hemispheric downward trend has  
55 been attributed to decreasing emissions from the North Atlantic Ocean due to decreasing mercury  
56 concentrations in subsurface water (Soerensen et al., 2012) and more recently to decreasing global  
57 anthropogenic emissions mainly due to the decline of mercury release from commercial products and  
58 the changes of Hg<sup>0</sup>/Hg<sup>2+</sup> speciation in flue gas of coal-fired utilities after implementation of NO<sub>x</sub> and  
59 SO<sub>2</sub> emission controls (Zhang et al., 2016). Mercury uptake by terrestrial vegetation has also been  
60 recently proposed to contribute to the downward trend (Jiskra et al., 2018).

61 In the meantime, mercury measurements at several other sites in the southern hemisphere have  
62 become available (Sprovieri et al., 2016, 2017). Atmospheric mercury is quite uniformly distributed  
63 throughout the southern hemisphere (Slemr et al., 2015) and its concentrations (~ 1.0 ng m<sup>-3</sup>) are  
64 substantially lower than those found at remote sites in the northern hemisphere (~1.5 ng m<sup>-3</sup>)  
65 (Sprovieri et al., 2016). Opposite to a pronounced seasonal variation with a maximum in early spring  
66 and a minimum in autumn in the northern hemisphere (Sprovieri et al., 2016), hardly any seasonal



67 variation has been observed at Cape Point and Amsterdam Island (Slemr et al., 2015). The absence of  
68 a pronounced seasonal variation in the southern hemisphere has been recently attributed to mercury  
69 uptake by the terrestrial vegetation which, due to land distribution, is smaller in the southern  
70 hemisphere (Jiskra et al., 2018).

71 In this paper we analyse the Cape Point (CPT) data for the 2007-2017 period and compare them with  
72 the data from Amsterdam Island (AMS) obtained in the years 2012-2017. Mercury concentrations  
73 remains nearly constant at both sites during the 2012 – 2017 period. Using simultaneously measured  
74  $^{222}\text{Rn}$ ,  $\text{CO}$ ,  $\text{O}_3$ ,  $\text{CO}_2$ , and  $\text{CH}_4$  concentrations at CPT and AMS we investigate the possible reasons for the  
75 trend and its change.

## 76 2 Experimental

77 The Cape Point station (CPT,  $34^\circ 21' \text{S}$ ,  $18^\circ 29' \text{E}$ ) is located on the southern tip of the Cape Peninsula  
78 within the Cape Point National Park at the summit of a 230 m a.s.l. peak about 60 km south of Cape  
79 Town. The site is operated as one of the Global Atmospheric Watch (GAW) baseline monitoring  
80 observatories of the World Meteorological Organisation (WMO) by South African Weather Service and  
81 its current continuous measurements include Hg,  $\text{CO}$ ,  $\text{O}_3$ ,  $\text{CH}_4$ ,  $\text{CO}_2$ ,  $^{222}\text{Rn}$ ,  $\text{N}_2\text{O}$ , several halocarbons,  
82 particles, and meteorological parameters (Martin et al., 2017).

83 Amsterdam Island (AMS,  $37^\circ 48' \text{S}$ ,  $77^\circ 34' \text{E}$ ) is a small island (55 km<sup>2</sup>) in the southern Indian Ocean,  
84 3400 km and 5000 km downwind of Madagascar and South Africa, respectively. The station is located  
85 at Pointe Bénédicte, at the northwest end of the island at an altitude of 55m a.s.l. Labelled GAW/WMO  
86 Global site, the Amsterdam site hosts instruments occurring in the framework of the French national  
87 observation service named ICOS-France-Atmosphere as well as the Global Observation System for  
88 Mercury (GOS4M), for long-term monitoring of greenhouse gases and mercury species, respectively.  
89 The site is ensured by the administration of Terres Australes and Antarctiques Françaises (TAAF), the  
90 French Southern and Antarctic Lands, and scientifically operated by the French Polar Institute (IPEV).  
91 Currently,  $\text{CO}$ ,  $\text{O}_3$ ,  $\text{CO}_2$ ,  $\text{CH}_4$ ,  $^{222}\text{Rn}$ , total aerosol number, carbonaceous aerosol, and meteorological  
92 parameters are continuously monitored at the site (Angot et al., 2014).

93 Atmospheric mercury has been measured since March 2007 at CPT and since January 2012 at AMS  
94 using Tekran 2537 (Tekran Inc., Toronto, Canada) at both sites. The instruments are based on mercury  
95 enrichment on a gold cartridge, followed by a thermal desorption and a detection by cold vapour  
96 atomic fluorescence spectroscopy (CVAFS). Switching between two cartridges allows for alternating  
97 sampling and desorption and thus results in a full temporal coverage of the mercury measurement.  
98 The instruments are automatically calibrated every 25 h at CPT and every 69 h at AMS using internal  
99 mercury permeation sources which in turn were annually checked by manual injections of saturated



100 Hg vapour from a temperature-controlled vessel. To ensure the comparability of the mercury  
101 measurements, Tekran instruments at both sites have been operated according to the Global Mercury  
102 Observation System (GMOS) standard operating procedures (SOP, Munthe et al., 2011).

103 The instrument at CPT has been operated with 15 min resolution since March 2007. At AMS, the Tekran  
104 speciation unit (Tekran 1130 and 1135) coupled to the Tekran 2537B analyser (Tekran Inc. Toronto,  
105 Canada) was in operation since January 2012 until December 10, 2015. Gaseous elemental mercury  
106 (GEM) was measured with 5 min resolution during this period. Concentrations of gaseous oxidized  
107 (GOM) and particulate mercury (PM) were below the detection limit for most of the time (Angot et al.,  
108 2014). Consequently, only GEM has been continuously measured with Tekran 2537A/B analyser since  
109 December 14, 2015, with a resolution of 15 min as at the Cape Point while GOM and PM species  
110 continued to be collected on CEM filters on weekly frequencies.

111 With GEM concentrations of  $\sim 1 \text{ ng m}^{-3}$  and a sampling flow rate of  $1 \text{ l (STP) min}^{-1}$  mercury loads on gold  
112 cartridges are  $\sim 5 \text{ pg}$  and  $\sim 15 \text{ pg}$  with 5 min and 15 min long sampling, respectively. A measurement  
113 bias with loads  $< 10 \text{ ng m}^{-3}$  due to internal Tekran integration procedure (Swartzendruber et al., 2009;  
114 Slemr et al., 2016a; Ambrose, 2017) can impair comparability of the measurements made with 5 min  
115 resolution with those made with 15 min resolution. The possible bias of the measurements at AMS in  
116 2012-2015 was eliminated by optimising the integration parameters (Swartzendruber et al., 2009). The  
117 absence of bias was shown by calculating the monthly variation coefficients of the 5 and the 15 min  
118 measurements at AMS. The average monthly variation coefficients were  $5.81 \pm 2.15 \%$  ( $n=48$ ) and  $5.83$   
119  $\pm 1.48 \%$  ( $n=24$ ) for 5 min and 15 min resolution, respectively, and they are statistically not  
120 distinguishable. We thus conclude that the measurements at AMS with 5 min resolution are  
121 comparable to those with 15 min.

## 122 **3 Results and discussion**

### 123 3.1 Seasonal variation

124 Figure 1 shows seasonal GEM variations at CPT (upper panel) and AMS (lower panel). They were  
125 calculated by averaging of monthly medians over the period of 2012 – 2017. Similar plots were  
126 obtained by averaging of monthly averages in the same period. The amplitude of the seasonal variation  
127 at AMS is with  $> 0.1 \text{ ng m}^{-3}$  somewhat larger than at CPT ( $\sim 0.08 \text{ ng m}^{-3}$ ). The standard deviations of  
128 monthly average concentrations are larger at CPT than at AMS indicating higher interannual variation  
129 at CPT. Smaller standard deviations at AMS enable to detect significant differences between the  
130 months with the highest (June, July, and August) and the lowest three (November, February, and  
131 October) GEM concentrations. GEM concentrations in December and January lie outside of an



132 otherwise nearly sinusoidal seasonal variation but their differences to GEM averages in other months  
133 are not significant. No significant differences between monthly averages at CPT were found.

134 In summary, maximum GEM concentrations at AMS are observed in austral winter (June – August) and  
135 the lowest GEM concentrations in austral summer. Austral winter is the season with the most frequent  
136 fast transport from southern Africa to AMS (June – October; Miller et al., 1993) coinciding also with  
137 maximum  $^{222}\text{Rn}$  concentrations at AMS (May – August) as another indicator of continental influence  
138 (Polian et al., 1986). The most frequent events at AMS in 1996 – 1997 with high CO mixing ratios  
139 occurred also in austral winter (June – October, Gros et al., 1999). Biomass burning in southern Africa  
140 peaks in austral winter (July – October, Duncan et al., 2003) and we therefore conclude, in agreement  
141 with Angot et al. (2014), that mercury from biomass burning in southern Africa combined with its fast  
142 transport to AMS is mostly responsible for the seasonal variation observed there. Reduced uptake of  
143 atmospheric GEM by terrestrial biomass of southern Africa in austral winter (Jiskra et al., 2018) can  
144 also contribute.

### 145 3.2 Trends at CPT in 2007 - 2017

146 Figure 2 shows annual median GEM concentrations at CPT (2007 – 2017) and at AMS (2012 – 2017).  
147 Table 1 shows the trends of GEM,  $\text{CO}_2$ ,  $^{222}\text{Rn}$ , CO,  $\text{CH}_4$ , and  $\text{O}_3$  at CPT in the 2007-2017 period as  
148 calculated by least square fit of monthly averages or medians (medians are shown in Figure 1 of  
149 Supporting Information). Monthly average and median GEM concentrations show a significant upward  
150 trend of  $7.69 \pm 2.11$  and  $7.01 \pm 2.11$   $\text{pg m}^{-3} \text{yr}^{-1}$ , respectively. The upward trends of  $\text{CO}_2$  ( $2.07 \pm 0.03$   
151  $\text{ppm yr}^{-1}$  for averages and  $2.08 \pm 0.02$   $\text{ppm yr}^{-1}$  for medians) and  $\text{CH}_4$  ( $5.70 \pm 0.66$   $\text{ppb yr}^{-1}$  for averages  
152 and  $5.85 \pm 0.53$   $\text{ppb yr}^{-1}$  for medians) are comparable to worldwide trends of  $2.24$   $\text{ppm yr}^{-1}$  for  $\text{CO}_2$  and  
153  $6.9$   $\text{ppb yr}^{-1}$  for  $\text{CH}_4$  in 2008-2017 (WMO Greenhouse Gas Bulletin, 2018). For the interpretation of the  
154 GEM trend, the most revealing is the non-significant trend in  $^{222}\text{Rn}$  and the significant downward trend  
155 in CO.  $^{222}\text{Rn}$  is a radioactive gas of predominantly terrestrial origin with a half-life of 3.8 days. Non-  
156 significant  $^{222}\text{Rn}$  trend thus implies a nearly constant ratio of oceanic to continental air masses over  
157 the 2007 – 2017 period and rules out larger shifts in climatology of CPT as the cause of the observed  
158 GEM trend. Biomass burning is a major source of CO in the southern hemisphere (Duncan et al., 2003;  
159 Pirrone et al., 2010) and at the same time a major source of Hg (Friedli et al., 2009). The downward  
160 trend of CO thus rules out increasing Hg emissions from biomass burning to be responsible for the  
161 upward GEM trend at CPT. The downward trend of CO at CPT is consistent with the decreasing CO  
162 emissions in 2001 – 2015 (Jiang et al., 2017). They report decreasing CO emissions from biomass  
163 burning from boreal North America, boreal Asia and South America and no change in Africa.

### 164 3.3 Trends at CPT and AMS in 2012 - 2017



165 Monthly GEM averages and medians at AMS and CPT in the 2012 - 2017 period are not statistically  
166 distinguishable according to the paired student t test. Monthly CO<sub>2</sub> averages at CPT are significantly  
167 higher than at AMS (at >99.9% significance level) but medians cannot be distinguished. Medians of  
168 CO<sub>2</sub>, <sup>222</sup>Rn, CO, and CH<sub>4</sub> are less influenced by occasional events with extremely high values and as such  
169 tend to be smaller than averages. Because such events are less frequent at AMS than at CPT, the  
170 differences between monthly averages and medians are always higher at CPT than at AMS. This  
171 explains why the CO<sub>2</sub> monthly averages are significantly higher at CPT than at AMS but the medians  
172 are not. Similarly, the significance of the monthly differences between higher CO at CPT and lower at  
173 AMS is >99.9% for averages but only >99% for medians. Monthly CH<sub>4</sub> mixing ratios are always higher  
174 at CPT than at AMS with >99.9% significance both for averages and medians. The most pronounced  
175 difference between CPT and AMS is in <sup>222</sup>Rn concentrations: monthly averages and medians at CPT are  
176 on average 16.6 and 12.6 times higher, respectively, than at AMS. In summary, higher monthly CO<sub>2</sub>,  
177 CO, CH<sub>4</sub>, and especially <sup>222</sup>Rn averages and medians at CPT than at AMS clearly demonstrate higher  
178 influence of continental air masses at CPT because all these species are predominantly of terrestrial  
179 origin. Statistically comparable GEM concentrations at AMS and CPT in 2012 – 2017, on the contrary,  
180 suggest that terrestrial GEM sources do not play a major role at CPT. This conclusion is supported by  
181 an analysis of GEM/<sup>222</sup>Rn ratios in events with enhanced <sup>222</sup>Rn concentrations observed at CPT (Slemr  
182 et al., 2013) which found terrestrial surface of southern Africa to be rather a sink of GEM than a source.  
183 This is further discussed in the companion paper (Bieser et al., 2019).

184 Tables 2 and 3 shows the 2012 – 2017 trends of GEM, CO<sub>2</sub>, <sup>222</sup>Rn, CO, and CH<sub>4</sub> at AMS and CPT,  
185 respectively. The AMS monthly average and median GEM concentrations do not show any significant  
186 trend. At CPT monthly average GEM concentrations do not show any significant trend, whereas median  
187 GEM concentrations show a significant slight downward trend (at >95% significance level). As in the  
188 2007-2017 period the neutral to slightly downward GEM trend at CPT is accompanied by no significant  
189 trend in <sup>222</sup>Rn. Opposite to the 2007 – 2017 period CO does not show any significant downward trend  
190 whereas O<sub>3</sub> (not listed) shows a small significant upward trend in monthly averages but not in monthly  
191 medians.

192 An inspection of Figure 2 shows that the GEM trend at CPT in 2007 – 2017 period is driven mainly by  
193 the 2009 – 2014 period. Table 1 of supporting information (SI) shows the trends of GEM, <sup>222</sup>Rn, CO,  
194 CH<sub>4</sub>, and O<sub>3</sub> at CPT for the 2007 – 2014 period. Monthly average and median GEM concentrations  
195 increased by  $16.91 \pm 3.60$  and  $16.18 \pm 3.61$  pg m<sup>-3</sup> yr<sup>-1</sup>, respectively. This upward GEM trend is  
196 accompanied by no trend in <sup>222</sup>Rn and O<sub>3</sub>, and small downward trend in monthly average CO mixing  
197 ratios but not in medians.



198 In summary, the 2007 – 2017 time series of GEM concentrations at CPT consists of two parts: one  
199 starting in 2007 and ending approximately in 2014 with a pronounced upward trend and the other  
200 without any or even slightly downward trend starting in 2012. The absence GEM trend in 2012 – 2017  
201 at CPT is in agreement with the absence of the GEM trend at AMS in the same period. The upward  
202 trend thus appears to have changed between 2012 and 2014. The absence of  $^{222}\text{Rn}$  trends at CPT for  
203 2007 – 2017 and the subperiods 2007 – 2014 and 2012 - 2017 points to nearly constant ratio of marine  
204 and continental air masses over the years and thus rules out shifts in regional climatology being  
205 responsible for the GEM trends. A downward trend of CO over the 2007 – 2017 period and none or  
206 just significantly downward one for the subperiods 2007 – 2014 and 2012 – 2017 makes it unlikely that  
207 increasing Hg emissions from biomass burning could be the reason for upward trend of GEM  
208 concentrations at CPT. We note that both  $^{222}\text{Rn}$  concentrations and CO mixing ratios have a very  
209 pronounced seasonal variations which make it difficult to determine significant trends over shorter  
210 periods.

#### 211 3.4 Inter-annual variations of GEM concentrations

212 A plot of annual median GEM concentrations in Figure 2 (annual averages provide a very similar pattern  
213 and are not shown) shows that median concentrations in 2007 and 2008 are only slightly lower than  
214 in 2015 - 2017. It is the steady increase from the lowest GEM concentrations in 2009 to the highest  
215 ones in 2014 at CPT (the latter 2<sup>nd</sup> highest at AMS in 2012 – 2017 period) which seems to be responsible  
216 for the upward trend in 2007 – 2017 at CPT and no trend for 2012 -2017 period for both CPT and AMS.  
217 Exceptionally low annual GEM concentrations in 2009 (average and median of 0.918 and 0.913 ng m<sup>-3</sup>,  
218 <sup>3</sup>, respectively) and exceptionally high ones in 2014 (average and median of 1.090 and 1.094 ng m<sup>-3</sup>,  
219 respectively, at CPT, 1.050 and 1.053 ng m<sup>-3</sup>, respectively, at AMS) seem to be a near global  
220 phenomenon. The years 2009 and 2014 show the largest deviations (a negative one in 2009, a positive  
221 one in 2014) from the linear 2000 - 2014 trend of annual GEM average concentrations recorded at 18  
222 sites in North America (Figure 8 b of Streets et al., 2019). At Mace Head, a site in Ireland, GEM annual  
223 average and median concentrations in 2009 were the lowest over the 1996 – 2013 period (supporting  
224 Information of Weigelt et al., 2015). The reasons for these near global inter-annual variations are not  
225 clear. Global anthropogenic Hg emissions do not vary much from year to year (mostly by less than 5%)  
226 and have been steadily increasing over the 2010 – 2015 period (Streets et al., 2019). Between 2000  
227 and 2010 they steadily increased by ~10% (Streets et al., 2017 and 2019). These emission estimates do  
228 not include Hg from biomass burning but CO emissions from biomass burning, as a proxy for Hg  
229 emissions, were somewhat lower in 2008 and 2009 but not exceptionally high in 2014 (Jiang et al.,  
230 2017). Annual volcanic SO<sub>2</sub> emissions, as a proxy for volcanic Hg emissions, also do not show  
231 exceptionally low emissions in 2009, although the emissions in 2014 were the second highest (after



232 2011) on record in the 1996 – 2018 period ([https://disc.gsfc.nasa.gov/datasets/MSVOLSQ2L4\\_V-](https://disc.gsfc.nasa.gov/datasets/MSVOLSQ2L4_V-3/summary)  
233 [3/summary](https://disc.gsfc.nasa.gov/datasets/MSVOLSQ2L4_V-3/summary)).

234 Tropospheric mercury concentrations were found to be influenced by El Niño Southern Oscillation  
235 (ENSO) (Slemr et al., 2016b). Such influence could also be a reason for the observed inter-annual  
236 variation of GEM concentrations at Cape Point. Table 4 shows correlations of 3 months running  
237 averages and medians of GEM concentration at CPT with 3 months running average of Southern  
238 Oscillation Index (SOI) for 2007 – 2014 and 2012 – 2017 and compares them with the 2012 – 2017  
239 period at AMS. 3 month running averages and medians were taken instead of monthly averages to  
240 take account for time of intra-hemispheric mixing. Correlations of CO mixing ratios with SOI  
241 ([www.cpc.ncep.noaa.gov/data/indices/soi.3m.txt](http://www.cpc.ncep.noaa.gov/data/indices/soi.3m.txt)) at CPT for 2007 – 2014 and 2012 – 2017 are also  
242 listed. CO vs SOI correlations for AMS were not made because the CO mixing ratios are available only  
243 since December 2015 until December 2017.

244  
245 Table 4 shows negative correlations of GEM concentrations with SOI at AMS for 2012 - 2017 with a lag  
246 of 6-8 months both for averages and medians. Relative GEM (after detrending) at CPT also  
247 anticorrelates with SOI at CPT in the 2007 – 2014 period as does CO mixing ratio (deseasonalised) in  
248 the same period, both with a slightly longer lag of 9 – 11 months. Anticorrelations of GEM  
249 concentrations and CO mixing ratios with SOI with similar lags were reported by Slemr et al. (2016b)  
250 who interpreted them as a sign for biomass burning being the driving force for the inter-annual  
251 variation of GEM and CO. The GEM and CO vs SOI correlations for the 2012 – 2017 period at CPT are  
252 both positive and the CO vs SOI correlation is significant only at >95% level. For the 2007 – 2017 period  
253 at CPT, encompassing both periods, also a negative correlation of GEM vs SOI was found but with a  
254 lower significance level of only >95%. The different correlations of GEM and CO with SOI at CPT for the  
255 period 2012 – 2017 from those at CPT in 2007 – 2014 and of GEM vs SOI at AMS in 2012 – 2017 clearly  
256 shows that at least at CPT the mechanism for inter-annual variations changed.

257 Correlations of detrended monthly GEM averages and medians at CPT with North Atlantic Oscillation  
258 (NAO) index  
259 ([www.cpc.ncep.noaa.gov/products/precip/Cwlink/pna/norm.nao.monthly.b5001.current.ascii.table](http://www.cpc.ncep.noaa.gov/products/precip/Cwlink/pna/norm.nao.monthly.b5001.current.ascii.table))  
260 over the period 2007 – 2017 were not significant for medians and just significant (>95%) for averages  
261 with a lag of 11 months. In the 2012 – 2017 period the correlations of GEM with NAO index were  
262 significant (>95%) with a delay of 0- and 8-months both for monthly medians and averages (both not  
263 detrended). The correlation with 0 months delay is negative and that with 8-month delay is positive.  
264 At AMS monthly GEM averages correlate with NAO index with a delay of 3, 5, and 6 months, all at a  
265 significance level of >95%. Monthly medians correlate with a delay of 5 and 6 months, the latter even





266 at a significance level of > 99%. In summary, there seems to be some influence of NAO on GEM  
267 concentration. The influence is more pronounced at AMS than at CPT, probably because of more  
268 regional influence at the latter site.

269 The annual GEM minimum in 2009 and the maxima in 2014 and 2012 at CPT as well as the annual  
270 minima in 2015 and 2017 and maxima in 2014 and 2016 at AMS fit a biennial tendency already  
271 mentioned by Martin et al. (2017) with mostly lower annual GEM concentrations in odd years and  
272 higher ones in even years. The biennial tendency is also apparent in the annual median and average  
273 CO mixing ratios at CPT (there are only two years with CO measurements at AMS), with mostly lower  
274 values in odd years and higher ones in even years, similar to GEM concentrations. Meehl and Arblaster  
275 (2001, 2002) note a relation between Tropospheric Biennial Oscillation (TBO) and ENSO, the latter also  
276 with a biennial tendency.

277 In summary, a part of the inter-annual variation of GEM concentrations seems to be related to  
278 teleconnections like ENSO, TBO and NAO.

## 279 **Conclusions**

280 Martin et al. (2017) reported an upward trend of GEM concentrations at CPT from March 2007 to June  
281 2015. With two and a half year of more measurements at CPT until December 2017 and GEM  
282 measurements at AMS since February 2012 until December 2017 a more complex picture emerged:

283 No significant trend of GEM concentrations was found at CPT and AMS for the period of AMS  
284 measurements, i.e. 2012 – 2017. Upward trend of GEM concentrations at CPT in 2007 – 2015 reported  
285 by Martin et al. (2017) is driven mainly by the 2009 – 2014 data with a minimum in 2009 and maxima  
286 in 2012 and 2014. The latter two years with high annual GEM concentrations seem to be the reason  
287 for absent trend in 2012 – 2017 period, although the upward trend over the whole 2007 – 2017 period  
288 at CPT is still significant. A minimum of GEM concentrations in 2009 was also reported for stations in  
289 North America and at Mace Head, Ireland. In addition, annual average and median GEM concentrations  
290 at CPT and AMS show a biennial pattern with lower concentrations in odd years and higher ones in  
291 even years. Because of the pronounced inter-annual variations, the calculated GEM trends will depend  
292 on the year when the observations start and end and increasingly so, the shorter the observation  
293 period is.

294 No trend was found in  $^{222}\text{Rn}$  concentrations and a slight downward trend in CO mixing ratios were  
295 found at CPT in 2007 – 2017. Changing ratios of marine and continental air masses at CPT as well as  
296 increasing mercury emissions from biomass burning can, therefore, be ruled out as the cause of the  
297 upward GEM trend at CPT.



298 Monthly average GEM concentrations at CPT and AMS in 2012 – 2017 are statistically indistinguishable  
299 while concentrations of species of terrestrial origin such as CO<sub>2</sub>, CH<sub>4</sub>, CO, and especially of <sup>222</sup>Rn clearly  
300 show substantially higher values at CPT in comparison with those at AMS. Comparable GEM  
301 concentrations at CPT and AMS despite much higher influence of terrestrial air masses at CPT thus  
302 indicate that terrestrial GEM sources are of minor importance and the oceanic GEM sources are  
303 dominating at CPT. This major conclusion will be substantiated by a companion paper in which the  
304 GEM concentration will be, with help of backward trajectories, attributed to different source and sink  
305 regions.

#### 306 References

307 Ambrose, J.L.: Improved methods for signal processing in measurements of mercury by Tekran 2537A  
308 and 2537B instruments, *Atmos. Meas. Tech.*, **10**, 5063-5073, 2017.

309 Angot, H., Barret, M., Magand, O., Ramonet, M., and Dommergue, A.: A 2-year record of atmospheric  
310 mercury species at a background Southern Hemisphere station on Amsterdam Island, *Atmos. Chem.  
311 Phys.*, **14**, 11461-11473, 2014.

312 Cole, A.S., Steffen, A., Eckley, C.S., Narayan, J., Pilote, M., Tordon, R., Graydon, J.A., Louis, V.L.St., Xu,  
313 X., and Branfireun, B.A.: A survey of mercury in air and precipitation across Canada: Patterns and  
314 trends, *Atmosphere*, **5**, 635-668, 2014.

315 Duncan, B.N., Martin, R.V., Staudt, A.C., Yevich, R., and Logan, J.A.: Interannual and seasonal variability  
316 of biomass burning emissions constrained by satellite observations, *J. Geophys. Res.*, **108**, D2, 4100,  
317 doi:10.1029/2002JD002378, 2003.

318 Friedli, H.R., Arellano, A.F., Cinnirella, S., and Pirrone, N.: Initial estimates of mercury emissions to the  
319 atmosphere from global biomass burning, *Environ. Sci. Technol.*, **43**, 3507-3513, 2009.

320 Jiang, Z., Worden, J.R., Worden, H., Deeter, M., Jones, D.B.A., Arellano, A.F., and Henze, D.K.: A 15-year  
321 record of CO emissions constrained by MOPITT CO observations, *Atmos. Chem. Phys.*, **17**, 4565-4583,  
322 2017.

323 Jiskra, M., Sonke, J.E., Obrist, D., Bieser, J., Ebinghaus, R., Lund Myhre, C., Pfaffhuber, K.A., Wängberg,  
324 I., Kyllönen, K., Worthy, D., Martin, L.G., Labuschagne, C., Mkololo, T., Ramonet, M., Magand, O., and  
325 Dommergue, A.: A vegetation control on seasonal variations in global atmospheric mercury  
326 concentrations, *Nature Geosci.*, **11**, 244-250, 2018.



- 327 Gros, V., Bonsang, B., Martin, D., Novelli, P.C., and Kazan, V.: Carbon monoxide short term  
328 measurements at Amsterdam Island: estimation of biomass burning emission rates, *Chemosphere*  
329 *Global Change Sci.*, **1**, 163-172, 1999.
- 330 Jiang, Z., Worden, J.R., Worden, H., Deeter, M., Jones, D.B.A., Arellano, A.F., and Henze, D.K.: A 15-year  
331 record of CO emission constrained by MOPITT CO observations, *Atmos. Chem. Phys.*, **17**, 4565-4583,  
332 2917.
- 333 Martin, L.G., Labuschagne, C., Brunke, E.-G., Weigelt, A., Ebinghaus, R., and Slemr, F.: Trend of  
334 atmospheric mercury concentrations at Cape Point for 1995-2004 and since 2007, *Atmos. Chem. Phys.*,  
335 **17**, 2393-2399, 2017.
- 336 Marumoto, K., Suzuki, N., Shibata, Y., Takeuchi, A., Takami, A., Fukuzaki, N., Kawamoto, K., Mizohata,  
337 A., Kato, S., Yamamoto, T., Chen, J., Hattori, T., Nagasaka, H., and Saito, M.: Long-term observation of  
338 atmospheric speciated mercury during 2007 – 2018 at Cape Hedo, Okinawa, Japan, *Atmosphere*, **10**,  
339 362, doi:10.3390/atmos10070362, 2019.
- 340 Meehl, G.A., and Arblaster, J.M.: The tropospheric biennial oscillation and Indian monsoon rainfall,  
341 *Geophys. Res. Lett.*, **28**, 1731-1734, 2001.
- 342 Meehl, G.A., and Arblaster, J.M.: The tropospheric biennial oscillation and Asian – Australian monsoon  
343 rainfall, *J. Climate*, **15**, 722-743, 2002.
- 344 Miller, J.M., Moody, J.L., Harris, J.M., and Gaudry, A.: A 10-year trajectory flow climatology for  
345 Amsterdam Island, 1980-1989, *Atmos. Environ.*, **27A**, 1909-1916, 1993.
- 346 Munthe, J., Sprovieri, F., Horvat, M., and Ebinghaus, R.: SOPs and QA/QC protocols regarding  
347 measurements of TGM, GEM, RGM, TPM and mercury in precipitation in cooperation with WP3, WP4,  
348 and WP5, GMOS deliverable 6.1, CNR-IIA, IVL, available at <http://www.gmos.eu> (last access on ), 2011.
- 349 Pirrone, N., Cinnirella, S., Feng, X., Finkelman, S.B., Friedli, H.R., Leaner, J., Mason, R., Mukherjee, A.B.,  
350 Stracher, G.B., Streets, D.G., and Telmer, K.: Global mercury emissions to the atmosphere from  
351 anthropogenic and natural sources, *Atmos. Chem. Phys.*, **10**, 5951-5964, 2010.
- 352 Polian, G., Lambert, G., Ardouine, B., and Jegou, A.: Long-range transport of continental radon in  
353 subantarctic and antarctic areas, *Tellus*, **38B**, 178-189, 1986.
- 354 Slemr, F., Brunke, E.-G., Whittlestone, S., Zahorowski, W., Ebinghaus, R., Kock, H.H., and Labuschagne,  
355 C.: <sup>222</sup>Rn-calibrated mercury fluxes from terrestrial surface of southern Africa, *Atmos. Chem. Phys.*, **13**,  
356 6421-6428, 2013.



- 357 Slemr, F., Angot, H., Dommergue, A., Magand, O., Barret, M., Weigelt, A., Ebinghaus, R., Brunke, E.-G.,  
358 Pfaffhuber, K.A., Edwards, G., Howard, D., Powell, J., Keywood, M., and Wang, F.: Comparison of  
359 mercury concentrations measured at several sites in the Southern Hemisphere, *Atmos. Chem. Phys.*  
360 15., 3125-3133, 2015.
- 361 Slemr, F., Weigelt, A., Ebinghaus, R., Kock, H.H., Bödeewadt, J., Brenninkmeijer, C.A.M., Rauthe-Schöch,  
362 A., Weber, S. Hermann, M., Becker, J., Zahn, A., and Martinsson, B.: Atmospheric mercury  
363 measurements onboard CARIBIC passenger aircraft, *Atmos. Meas. Tech.*, 9, 2291-2302, 2016a.
- 364 Slemr, F., Brenninkmeijer, C.A., Rauthe-Schöch, A., Weigelt, A. Ebinghaus, R., Brunke, E.G., Martin, L.,  
365 Spain, T.G., and O 'Doherty, S.: El Niño-Southern Oscillation influence on tropospheric mercury  
366 concentrations, *Geophys. Res. Lett.*, 43, 1766-1771, 2016b.
- 367 Soerensen, A.L., Jacob, D.J., Streets, D.G., Witt, M.L.I., Ebinghaus, R., Mason, R.P., Andersson, M., and  
368 Sunderland, E.M.: Multi-decadal decline of mercury in the North Atlantic atmosphere explained by  
369 changing subsurface seawater concentrations, *Geophys. Res. Lett.*, 39, L21810,  
370 doi:10.1029/2012GL053736, 2012.
- 371 Sprovieri, F., Pirrone, N, Bencardino, N., D'Amore, F., Carbone, F., Cinnirella, S., Mannarino, V., Landis,  
372 M., Ebinghaus, R., Weigelt, A., Brunke, E.-G., Labuschagne, C., Martin, L., Munthe, J., Wängberg, I.,  
373 Artaxo, P., Morais, F., de Melo Jorge Barbosa, H., Brito, J., Cairns, W., Barbante, C., del Carmen Diéguez,  
374 M., Garcia, P.E., Dommergue, A., Angot, H., Magand, O., Skov, H., Horvat, M., Kotnik, J., Read, K.A.,  
375 Mendes Leves, L., Gawlik, B.M., Sena, F., Mashyanov, N., Obolkin, V., Wip, D., Feng, X.B., Zhang, H., Fu,  
376 X., Ramachandran, R., Cossa, D., Knoery, J., Maruszczak, N., Nerentorp, M., and Norstrom, C.:  
377 Atmospheric mercury concentrations observed at ground-based monitoring sites globally distributed  
378 in the framework of the GMOS network, *Atmos. Chem. Phys.*, 16, 11915-11935, 2016.
- 379 Sprovieri, F., Pirrone, N, Bencardino, N., D'Amore, F., Angot, H., Barbante, C., Brunke, E.-G., Arcega-  
380 Cabrera, F., Cairns, W., Comero, S., del Carmen Diéguez, M., Dommergue, A., Ebinghaus, R., Feng, X.B.,  
381 Fu, X., Garcia, P.E., Gawlik, P.M., Hageström, U., Hansson, K., Horvat, M., Kotnik, J., Labuschagne, C.,  
382 Magand, O., Martin, L., Mashyanov, N., Mkololo, T., Munthe, J., Obolkin, V., Ramirez Islas, M., Sena, F.,  
383 Somerset, V., Spandow, P., Vardè, M., Walters, C., Wängberg, I., Weigelt, A., Yang, X., and Zhang, H.:  
384 Five-year records of mercury deposition flux at GMOS sites in the Northern and Southern hemispheres,  
385 *Atmos. Chem. Phys.*, 17, 2689-2708, 2017.
- 386 Steffen, A., Lehnher, I., Cole, A., Ariya, P., Dastoor, A., Durnford, D., Kirk, J., and Pilote, M.:  
387 Atmospheric mercury in the Canadian Arctic. Part I: A review of recent field measurements, *Sci. Tot.*  
388 *Environ.*, 509-510, 3-15, 2015.



389 Streets, D.G., Horowitz, H.M., Jacob, D.J., Lu, Z., Levin, L., ter Schure, A.F.H., and Sunderland, E.M.:  
390 Total mercury released to the environment by human activities, *Environ. Sci. Technol.*, 51, 5969-5977,  
391 2017.

392 Streets, D.G., Horowitz, H.M., Lu, Z., Levin, L., Thackray, C.P., and Sunderland, E.M.: Global and regional  
393 trends in mercury emissions and concentrations, 2010 – 2015, *Atmos. Environ.*, 201, 417-2015, 2019.

394 Swartzendruber, P.C., Jaffe, D.A., and Finley, B.: Improved fluorescence peak integration in the Tekran  
395 2537 for applications with sub-optimal sample loadings, *Atmos. Environ.*, 43, 3648-3651, 2009.

396 Temme, C., Blanchard, P., Steffen A., Banic, C., Beauchamp, S., Poissant, L., Tordon, R., and Wiens, B.:  
397 Trend, seasonal and multivariate analysis study of total gaseous mercury data from the Canadian  
398 atmospheric mercury measurement network (CAMNet), *Atmos. Environ.*, 41, 5423-5441, 2007.

399 Weigelt, A., Ebinghaus, R. Manning, A.J., Derwent, R.G., Simmonds, P.G., Spain, T.G., Jennings, S.G.,  
400 and Slemr, F.: Analysis and interpretation of 18 years of mercury observations since 1996 at Mace  
401 Head, Ireland, *Atmos. Environ.*, 100, 85-93, 2015.

402 Weiss-Penzias, P.S., Gay, D.A., Brigham, M.E., Parsons, M.T., Gustin, M.S., and ter Schure, A.: Trends in  
403 mercury wet deposition and mercury air concentrations across the U.S. and Canada, *Sci. Tot. Environ.*,  
404 568, 546-556, 2016.

405 WMO Greenhouse Gas Bulletin, No. 14, 22 November 2018.

406 Zhang, Y., Jacob, D.J., Horowitz, H.M., Chen, L., Amos, H.M., Krabbenhoft, D.P., Slemr, F., Louis, V.L.St.,  
407 and Sunderland, E.M.: Observed decrease in atmospheric mercury explained by global decline in  
408 anthropogenic emissions, *PNAS*, 113, 526-531, 2016.

409

410



411 **Tables**

412 *Table 1. Trends at Cape Point for the 2007 – 2017 period. Calculated by LSQF from monthly*  
413 *averages and medians.*

Species	Monthly	Annual slope	Unit	R, n, significance
GEM	average	$7.69 \pm 2.11$	$\text{pg m}^{-3} \text{ yr}^{-1}$	0.3098, 127, >99.9%
	median	$7.01 \pm 2.11$		0.2846, 127, >99%
CO <sub>2</sub>	average	$2.208 \pm 0.018$	ppm yr <sup>-1</sup>	0.9955, 132, >99.9%
	median	$2.219 \pm 0.017$		0.9964, 132, >99.9%
Rn	average	$-0.76 \pm 7.96$	$\text{mBq m}^{-3} \text{ yr}^{-1}$	-0.0085, 130, ns
	median	$0.05 \pm 4.58$		0.0009, 130, ns
CO	average	$-1.020 \pm 0.301$	ppb yr <sup>-1</sup>	-0.2848, 132, >99%
	median	$-0.503 \pm 0.223$		-0.1939, 132, >95%
CH <sub>4</sub>	average	$6.650 \pm 0.402$	ppb yr <sup>-1</sup>	0.8236, 132, >99.9%
	median	$6.895 \pm 0.335$		0.8751, 132, >99.9%
O <sub>3</sub>	average	$0.263 \pm 0.151$	ppb yr <sup>-1</sup>	0.1510, 131, ns
	median	$0.260 \pm 0.161$		0.1408, 131, ns

414

415



416 *Table 2: Trends at Amsterdam Island for the 2012 - 2017 period.*

Species	Monthly	Annual slope	Unit	R, n, significance
GEM	average	$4.10 \pm 3.65$	$\text{pg m}^{-3} \text{ yr}^{-1}$	0.1371, 68, ns
	median	$5.57 \pm 3.61$		0.1865, 68, ns
CO <sub>2</sub>	average	$2.487 \pm 0.025$	ppm yr <sup>-1</sup>	0.9962, 72, >99.9%
	median	$2.487 \pm 0.026$		0.9959, 72, >99.9%
Rn	average	$-1.626 \pm 1.018$	$\text{mBq m}^{-3} \text{ yr}^{-1}$	-0.190, 70, ns
	median	$-0.557 \pm 0.604$		-0.111, 70, ns
CO	average	$-1.530 \pm 2.405$	ppb yr <sup>-1</sup>	-0.131, 25, ns
	median	$-1.460 \pm 2.351$		-0.128, 25, ns
CH <sub>4</sub>	average	$8.575 \pm 0.786$	ppb yr <sup>-1</sup>	0.7932, 72, >99.9%
	median	$8.555 \pm 0.793$		0.7899, 72, >99.9%

417

418 *Table 3. Trends at Cape Point for the 2012 – 2017 period.*

Species	Monthly	Annual slope	Unit	R, n, significance
GEM	average	$-8.65 \pm 4.63$	$\text{pg m}^{-3} \text{ yr}^{-1}$	-0.2211, 70, ns
	median	$-9.31 \pm 4.55$		-0.2409, 70, >95%
CO <sub>2</sub>	average	$2.459 \pm 0.035$	ppm yr <sup>-1</sup>	0.9931, 72, >99.9%
	median	$2.466 \pm 0.030$		0.9949, 72, >99.9%
Rn	average	$20.05 \pm 18.87$	$\text{mBq m}^{-3} \text{ yr}^{-1}$	0.1269, 71, ns
	median	$15.36 \pm 10.51$		0.1732, 71, ns
CO	average	$-0.151 \pm 0.692$	ppb yr <sup>-1</sup>	-0.0260, 72, ns
	median	$0.053 \pm 0.540$		0.0117, 72, ns
CH <sub>4</sub>	average	$9.160 \pm 0.979$	ppb yr <sup>-1</sup>	0.7455, 72, >99.9%
	median	$9.498 \pm 0.818$		0.8111, 72, >99.9%

419

420



421 Table 4: Correlation of 3 months running average and median GEM concentrations and CO  
 422 mixing ratios with 3 months running average of SOI  
 423 ([www.cpc.ncep.noaa.gov/data/indices/soi.3m.txt](http://www.cpc.ncep.noaa.gov/data/indices/soi.3m.txt)). The CPT GEM data for 2007 – 2014 were  
 424 detrended, the CPT CO data for 2007-2014 and 2012-2017 deseasonalized using the average  
 425 monthly averages or medians over the period. No CO correlation is presented for AMS  
 426 because CO data are available only since December 2015 until December 2017. The delay  
 427 given in the last column is the one with the highest R. The delays in the brackets are  
 428 significant correlations with the second and third highest R.

429

Site and period		Equation	R, n, signif.	GEM delay [month]
AMS, GEM, 2012–2017	average	$GEM = -0.0227 * SOI + 1.0375$	-0.4145, 70, >99.9%	7 (6-8)
	median	$GEM = -0.0230 * SOI + 1.0390$	-0.4150, 70, >99.9%	7 (6-8)
CPT, GEM, 2007-2014	average	$relGEM = -0.0330 * SOI + 1.0179$	-0.4554, 95, >99.9%	10 (9-11)
	median	$relGEM = -0.0373 * SOI + 1.0202$	-0.4934, 95, >99%	10 (9-11)
CPT, CO, 2007-2014	average	$relCO = -0.0367 * SOI + 1.0199$	-0.4171, 95, >99.9%	10 (9-11)
	median	$relCO = -0.0340 * SOI + 1.0184$	-0.5406, 95, >99.9%	10 (9-11)
CPT, GEM, 2012-2017	average	$GEM = 0.0318 * SOI + 1.0371$	0.4523, 69, >99.9%	8 (7-9)
	median	$GEM = 0.0279 * SOI + 1.0385$	0.3906, 69, >99.9%	7 (7-9)
CPT, CO, 2012-2017	average	$relCO = 0.0173 * SOI + 0.9995$	0.2358, 71, >95%	8 (9)
	median	$relCO = 0.0196 * SOI + 0.9991$	0.2914, 71, >95%	9 (10-11)

430

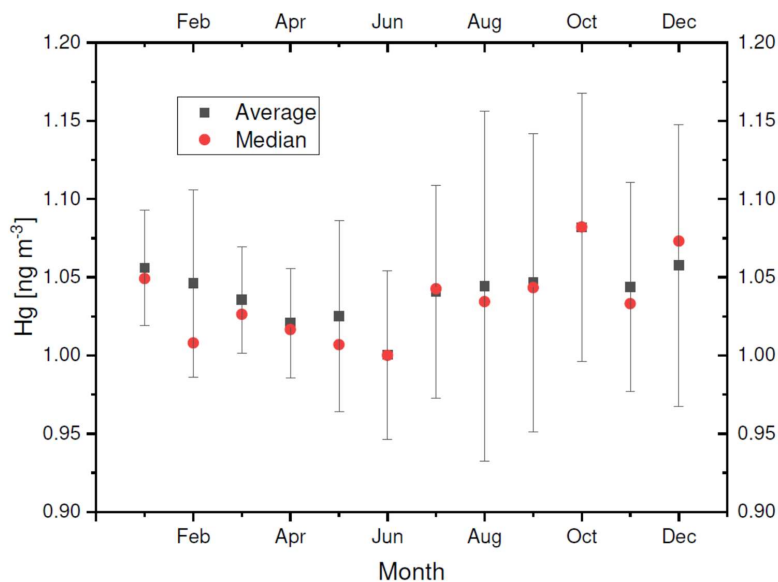
431



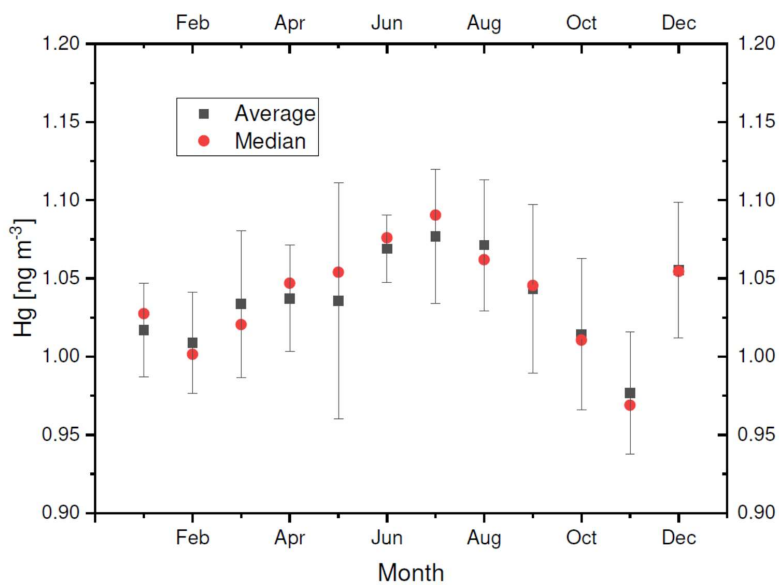


432 **Figures**

433



434

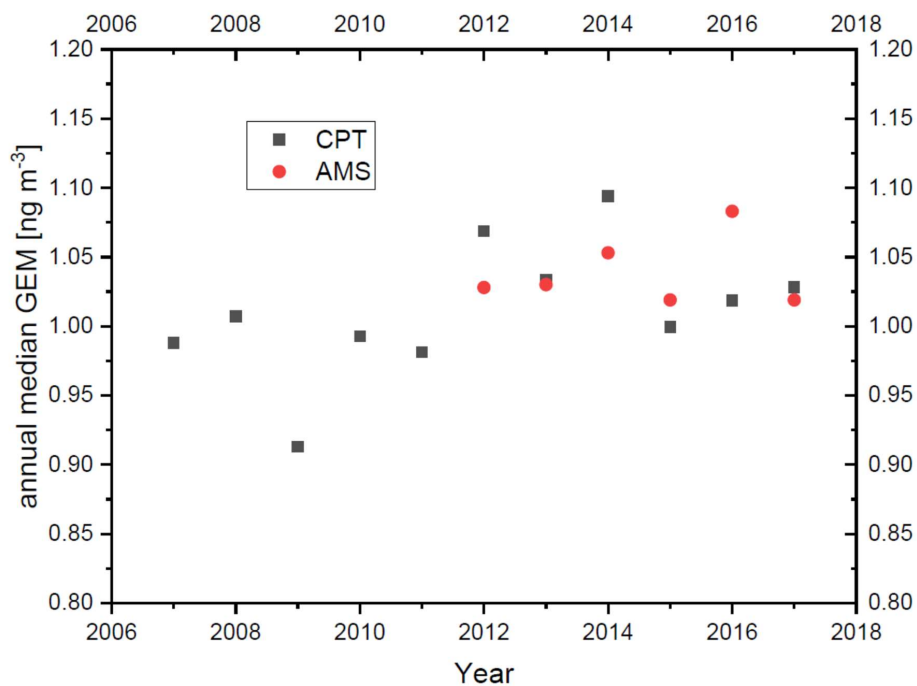


435

436 Figure 1: Seasonal variation of GEM in 2012 – 2017 at CPT (upper panel)  
437 and AMS (lower panel). The points represent averages and medians of monthly  
438 medians over the 2012 – 2017 period. The bars represent the standard deviations  
of the monthly averages.



439



440

441

442 Figure 2: Annual median GEM concentrations at Cape Point (CPT) since March 2007 until  
443 December 2017 and at Amsterdam Island (AMS) since February 2012 until December 2017.

444